

The main role of fractal-like nature of conformational space in subdiffusion in protein

Luca Maggi

Mechanisms of Diseases, Institute for Research in Biomedicine (IRB Barcelona), The Barcelona Institute of Science and Technology, Baldori Reixac 10-12, Barcelona 08028, Spain

e-mail address: luca.maggi@irbbarcelona.org

Abstract:

Protein dynamics is a fundamental element to comprehend their biological functions. However, a theoretical picture providing microscopic-detail explanation of its relevant features is still missing. One of the outmost relevant properties exhibited by this dynamic is its subdiffusivity, whose origins are still unknown. Here, by directly comparing all-atom molecular dynamics simulations and theory we show that this behavior mainly arises from the fractal nature of the network of metastable state of conformational state over which protein dynamics, thought as diffusion process, takes place. This process is assumed to be Markovian by the employed theoretical picture. Therefore, to further support its validity, we built a simple Markov state model starting from the simulations outcome and show that it exhibits a subdiffusive behavior, in quantitative agreement with the one associated to the molecular dynamics. Moreover, Molecular dynamics gives direct access to relevant quantities which allowed us to rule out the possibility the Continuous Time Random Walk can explain the protein subdiffusivity.

Main text:

A fundamental paradigm in structural biology stated the relationship between protein structure and function. However, aside a single specific arrangement of protein atoms (i.e., a conformation), the dynamics is widely being recognized as a pivotal element to understand protein function at microscopic level [1,2]. Catalytic enzymatic reactions [3], signal transduction [4] and molecule transport across the plasmatic membrane [5] are significant examples in which protein dynamics plays a crucial role and, thus, its investigation cannot thus be neglected. To avoid any source of confusion here we refer to protein dynamics as every time-dependent change of protein conformation. This is determined by the interactions that residues have with each other and with external environment. The whole set of those produces a potential energy landscape whose explicit analytical treatment is, however, unfeasible mainly due to its high dimensionality and complexity. Nevertheless, experimental and computational studies highlighted some of its relevant features as the inherently “roughness” which gives rise to a conformational space composed by a plenty of metastable states separated by energy barriers of different heights [1,2,6]. According to this picture, therefore, protein dynamics is often modeled as a diffusion process among those metastable states [7–9], the same model is adopted in the present work. Previous investigations directly and indirectly showed [8,10–14] that the diffusion process exhibits a subdiffusive behavior, which implies a sublinear relationship between the mean

square displacement (MSD) and time. More formally speaking, if $X(t) = \{x_1(t), \dots, x_N(t)\}$ is a single conformation, with $x_i(t)$ the i -th degree of freedom at time t and N the total number of degrees of freedom, it follows:

$$MSD = \langle |X(0) - X(t)|^2 \rangle \sim t^\alpha \quad (\text{Eq. 1})$$

Where $\langle \dots \rangle$ represents an ensemble average. In Eq. 1 subdiffusivity imposes α to be smaller than 1. Despite numerous and notably theoretical efforts [14–17] the microscopic origin of this phenomenon is still unclear. In this letter we bring strong evidences that indicates the fractal nature of the protein conformational space as the main origin of subdiffusion in protein. This is achieved by employing all atom Molecular Dynamics (MD) simulations to directly verify theoretical results. The theory which describes a diffusion process on a fractal structure prescribes that exponent α is given by [18,19]:

$$\alpha = \frac{d_s}{d_f} \quad (\text{Eq. 2})$$

Where d_f is associated to geometrical properties of conformational space and d_s is related to spectral features of the operator generating the diffusion process [18,19]. Our goal is, therefore, to calculate α , d_f , and d_s separately and verify whether Eq. 2 holds. The evaluation of those three quantities has been achieved by the analysis of 1- μ s MD simulations of three biomolecules: the N-terminal of the human histone H4 tail (H4); The Villin headpiece (Villin; PDB ID: 1VII [20]) and a PDZ domain (PDZ; PDB ID: 1D5G [21]), Fig. 1a-c. They differ for the number of residues, which are: 25, 32 and 96 for H4, Villin and PDZ respectively, and its secondary and tertiary structure as H4 is a totally disordered peptide, Villin exhibits a partial structure and the PDZ can be classified as a small globular structured protein. All the MD simulations details are given in SI. In order to reduce the number of degrees of freedom we projected all the trajectories on to the first two principal component extracted from a principal component analysis, PC1(t) and PC2(t), carried out taking into account C α 's backbone only. Hence, those two variables define a single sampled conformation, $X(t) = \{PC1(t), PC2(t)\}$. The identification of metastable states has been done over this sub-space by means of a clustering algorithm. In this work an agglomerative hierarchical clustering method is employed [22]. The reasons leading to this choice are two-fold. Firstly, the intrinsic hierarchy of the whole metastable states appears reasonable as structural differences among conformations can be naturally classified as sub-sets of decreasing size which sub-divide the entire space. This idea is supported by previous works which highlighted this feature [2,7]. On the other hand, this clustering method presents technical advantages as it does not require to set a fixed number of clusters (as K-means methods) employing an adjustable parameter that controls the cluster average size (ϵ) and it does not produce any outlier conformations which are hard to be included in the theoretical picture. The dynamics including each single conformation is, thus, replaced by a coarse-grained one involving only the cluster centroids which correspond to the representative conformations of each single metastable state. The average cluster size, is chosen to reproduce at the best the MSD calculated from fine-grained conformational sub-space, still providing a reliable sampling of each cluster (see Fig SI 1). The MSD calculation are performed using a moving average to cancel out the dependence from the initial conditions, and it reads:

$$MSD = \frac{1}{T-t} \int_0^{T-t} d\tau |X(t+\tau) - X(\tau)|^2 \quad (\text{Eq. 3})$$

Where $t < 0.01 T$, where T is maximum simulation time (1us). We found that setting ε within a range from 1.0 to 0.2, depending on the system, produces almost the same subdiffusive behavior as showed by the very small relative difference between the exponent α 's evaluated in the two cases, (reported as percentage) $\Delta = \frac{|\alpha - \alpha_{fine}|}{\alpha_{fine}}$, where α and α_{fine} are the exponents calculated for coarse- and fine-grained conformational space respectively (Fig 1d–f). The distribution of metastable states over the sub-space is connected to d_f which relates the number of cluster centroids within a sphere of radius r , $M(r)$, to the radius itself as, $M(r) \sim r^{d_f}$. The $M(r)$ profiles are evaluated averaging over all the clusters and presented in Fig. 2a-c. All of them exhibit a power law relation with d_f always less than 2 showing the non-homogenous distribution of cluster centroids. While d_f is associated with the geometric arrangement of metastable states in the conformational sub-space, d_s is related to their “connectivity”, determining the spectral density of the operator generating the diffusion process [23]. Employing an operative definition this exponent characterizes the probability of a trajectory to return to its starting point (P_o) after a time t , being $P_o \sim t^{-d_s/2}$. In our case the “starting point” coincides with the starting metastable states (i.e., starting cluster). Hence, we introduced $C(t+\tau, \tau)$ which is a function equal to 1 if the cluster visited at $t+\tau$ and τ are the same and 0 otherwise and P_o is calculated employing a moving average:

$$P_o(t) = \frac{1}{T-t} \int_0^{T-t} d\tau C(t+\tau, \tau) \quad (\text{Eq. 4})$$

The profiles show a good agreement with power-law relation within about four order of magnitude (Fig. 2 d-f). In Tab.1 we summarize all the calculated quantities and compare the subdiffusion exponent α with d_s/d_f . We found an excellent quantitative agreement between these two. Therefore, it turns out that the theory of diffusion on fractals is capable to adequately modeling the protein conformational space exploration as described by all atom Molecular dynamics simulations and it should be noticed the general validity of this finding as it holds for biomolecules which present very different structural features. This is the main result of this work.

Interestingly, the correspondence between theory and simulations entails an important feature of diffusion process which is its Markovianity [19]. Therefore, to test this implication we have extracted a transition probability matrix (T) directly from the MD simulations and analyzed the MSD resulting from this Markov state model (MSM). The matrix T is $N_c \times N_c$ matrix, where N_c is the total number of clusters, and each element T_{ij} is equal to:

$$T_{ij} = \frac{s_{ij}}{\sum_{i=1}^{N_c} s_{ij}} \quad (\text{Eq. 5})$$

Where s_{ij} is the number of “jumps” between the i -th and j -th cluster. Obviously, the finiteness and discreteness of T prevents the results to arbitrarily coincide with the MD results which are, instead, produced by an infinite and continuous operator [24]. To each cluster has been assigned a stationary

probability value (π_s) extracted directly from the simulations and system time evolution consist in the evolution of the N_c -length probability vector $\boldsymbol{\pi}$, which evolves like a time discrete Markov chain and at each step n we can calculate this vector for the step $n+1$ as:

$$\boldsymbol{\pi}_{n+1} = T \boldsymbol{\pi}_n \quad (\text{Eq. 6})$$

Therefore, the MSD in this case has been calculated as:

$$MSD = \Delta t \cdot \sum_{i=1}^{N_c} \sum_{j=1}^{N_c} \pi_s^i \cdot \pi_n^j d_{ij}^2 \quad (\text{Eq. 7})$$

Where Δt is the smallest sampling step in MD simulations (20 ps, see SI). The apices i, j indicates the relative cluster and d_{ij}^2 is the square distance between them. Despite the unavoidable flaws introduced in the presented MSM, the calculated MSD exhibits a very similar quantitative time dependence to the one associated to MD simulations (Fig 3). This supports further the main finding and gives a new impetus to the debate over the long-memory effect on protein dynamics which has been previously accounted for to model the diffusion process in the conformational space. One of the most common microscopic theoretical pictures involving memory effects is the continuous time random walk (CTRW) which describes the diffusion as time-continuous jumping process among metastable states separated by energy barriers which, to give rise a subdiffusive dynamics, are distributed according to a power-law. This produces a sub-linear time relationship for the average number of jumps $\langle N(t) \rangle \sim t^\alpha$ which originates subdiffusion [25]. To show that the subdiffusivity shown in all atom MD simulations cannot be described by CTRW we have directly calculated $\langle N(t) \rangle$ as:

$$\langle N(t) \rangle = \int_0^t d\tau |C(\tau + \Delta t, \tau) - 1| \quad (\text{Eq. 8})$$

This quantity shows a time linear dependence independently from the size of clusters (Fig 4a). Moreover, the probability of “observing a jump within a time t , presents an exponential decay since its profile doesn’t show any region following a power law relationship which should be invariant upon cluster size changing (Fig 4b). Therefore, the evaluation of those two quantities rules out CTRW as a possible description of subdiffusivity observed in all atom MD simulations.

In conclusion we brought compelling evidence that subdiffusive protein dynamics, as described by MD simulations, stems from the fractal nature of the conformational space. The high dimensional and rough potential energy landscape gives rise to separated basins of attractions, namely metastable states whose distribution in the conformational space, regulated by d_f , resembles a fractal structures. On the other hand, d_s is related to the connections among those states modulating the accessibility from one to another. The whole dynamics is therefore described by these two exponents which are directly connected to the geometry of the conformational energy landscape. As corollary we also highlighted the parallelism between the diffusion and a Markov process as implied by theory of diffusion on fractals and ruled out the role of CTRW in the origin of subdiffusion phenomenon.

Figures:

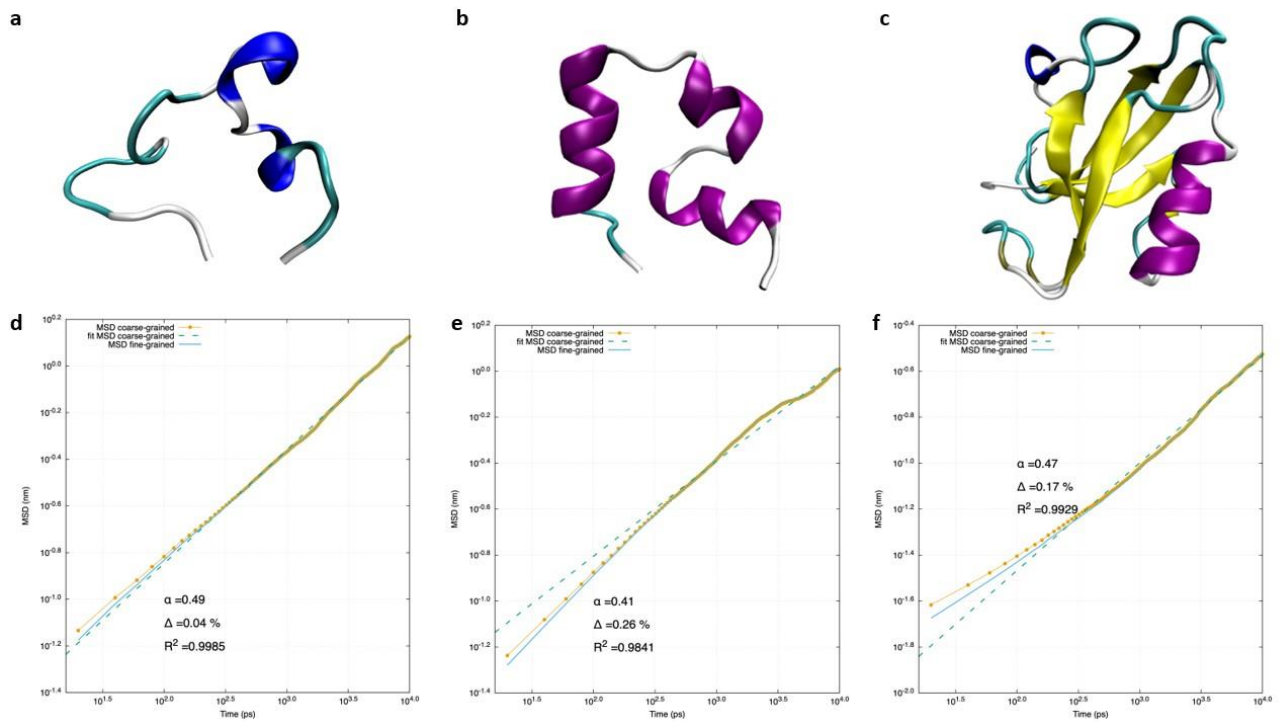


Fig 1: Snapshot extracted from MD simulations of the three investigated systems and the associated MSD linearly fitted: a-d) H4 tail, b-e) Villin, c-f) PDZ domain and

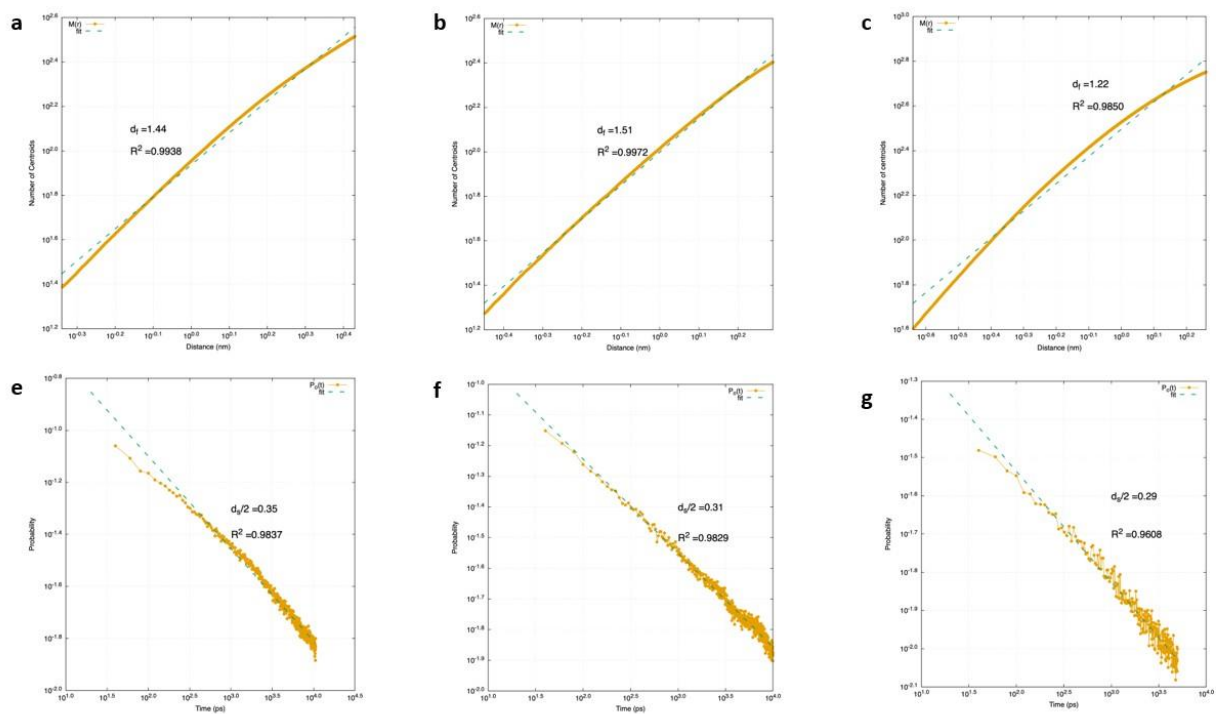
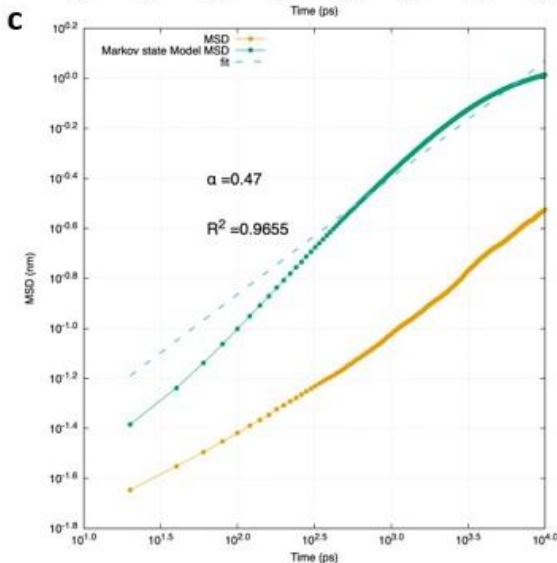
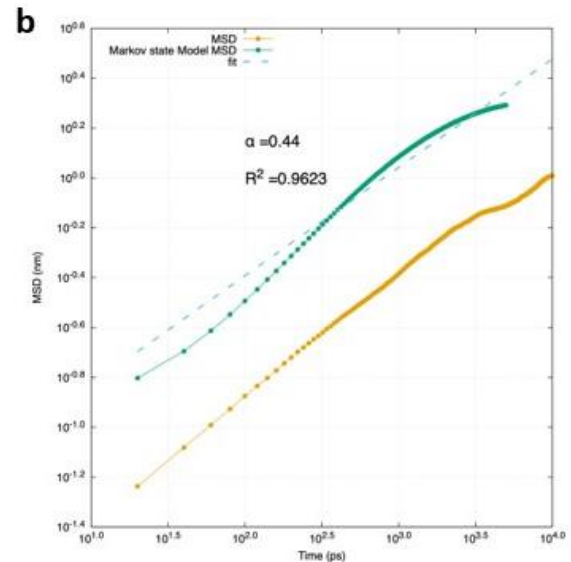
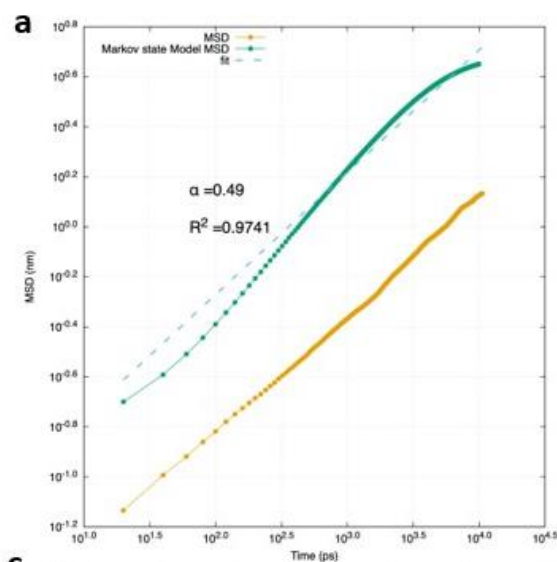


Fig 2: $M(r)$ and $P_0(t)$ profile and the associated linear fit for the three systems: a-d) H4 tail, b-e) Villin, c-f) PDZ domain. The radius value range within which the $M(r)$ linear fit has been performed,

corresponds to 5% and 70 % of the total number of metastable states, to avoid artifacts due to the conformational space discreteness and finiteness

System	d_f	d_s	$\alpha = d_s/d_f$	α_{fit}
H4	1.44	0.70	0.486	0.49
Villin	1.51	0.62	0.411	0.41
PDZ	1.22	0.58	0.475	0.47

Tab 1: Summarizing table showing all the evaluated exponents for all the system under investigation and comparing the α coming from the theory and extracted directly from the fit with MSD (α_{fit}).



System	α_{fit}	α_{MSM}
H4	0.49	0.49
Villin	0.41	0.44
PDZ	0.48	0.47

Fig. 3: Comparison between Markov state model MSD and the one calculated from MD simulations for the Different systems investigated: a) H4 tail, b) Villin, c) PDZ d) Summarizing table

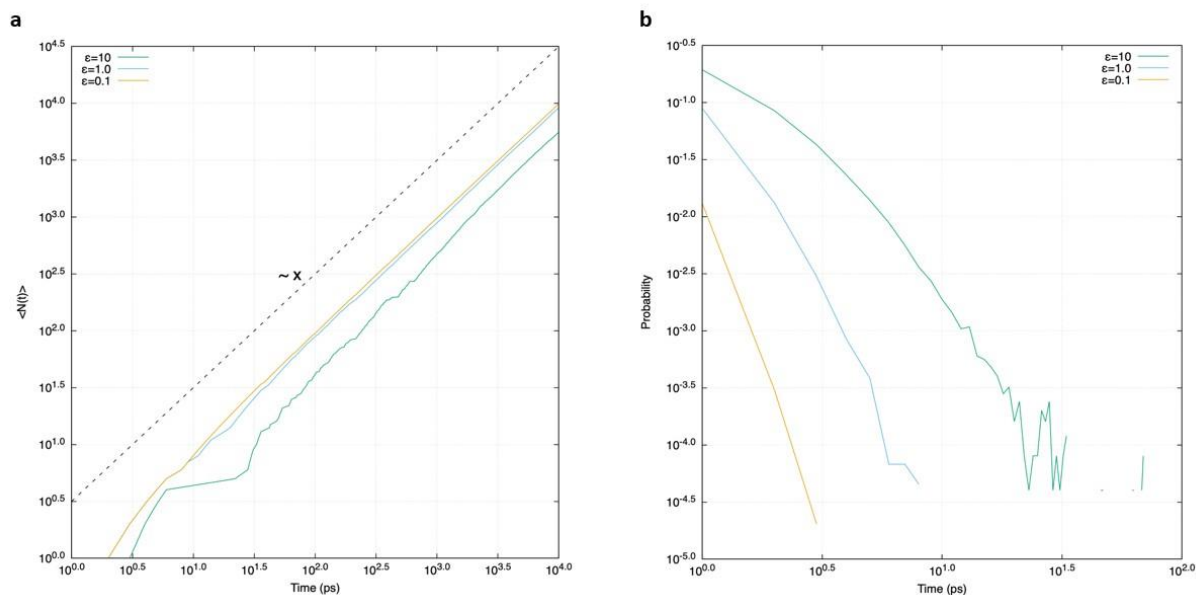


Fig. 4: a) $\langle N(t) \rangle$ and b) probability of jumps for Villin with three different average cluster size. The linear profile for $\langle N(t) \rangle$ as well as the exponential decay for probability of jump are conserved feature upon changing the cluster size. H4 and PDZ plots exhibit the same characteristics (Fig. SI 2).

Supporting Information:

Molecular Dynamics details

All the presented simulations are carried out with following procedure. The simulations boxes which presented different sizes: 40x40x40, 47x47x47, 69x69x69 Å³ for H4, Villin and PDZ respectively are filled with TIP3P water molecules and Na⁺ and Cl⁻ atoms to neutralize the systems. A first 100 ns equilibration step has been run followed by 1- μ s production run from which has been extracted frames every 20 ps. LINCS [26] was used to constrain all the bonds involving hydrogens allowing us to employ a 2 fs step to integrate the Newton equations. The first equilibration part is divided into 50 ns NVT ensemble simulation where T=310K, followed by a 50 ns NPT ensemble run to set the total pressure to 1 atm. We employed a Berendsen thermostat [27] {Ref.} with a coupling constant of 0.4 ps for the NVT ensemble and a Nose-Hover [28] {ref.} thermostat along with a Parrinello-Rahman Barostat [29] with 0.4 and 0.6 ps coupling constant respectively for the NPT ensemble, which are used also for the production run. We employed Mesh Ewald method to account for long-range interactions with a real-space cut-off of 12 Å. We used GROMAC 2020.2 [30] code with Amber99sb-ildn force field for all the simulation.

Molecular Dynamics Analysis:

All the linear fit presented in this work has been done with Gnuplot 5.4. Python Scikit Learn suite [31] is employed for the hierarchical clustering using a Word linkage method. The rest of the analysis are carried out utilizing *ad hoc* in-house scripts.

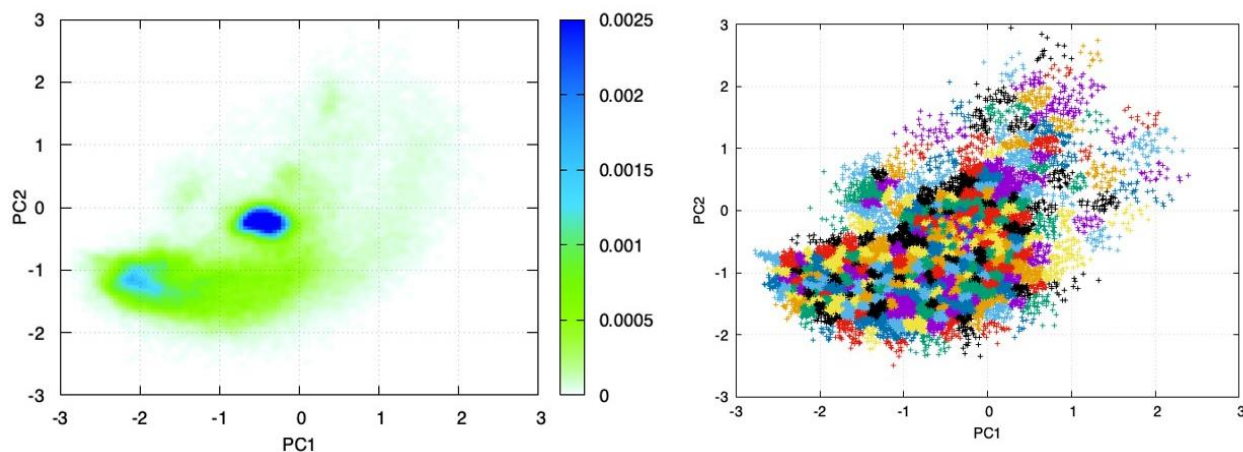


Fig. SI 1: Villin free energy surface projected on to PC1 and PC2 on left. On right the same surface is subdivided into clusters identified by hierarchical clustering as described in the main text

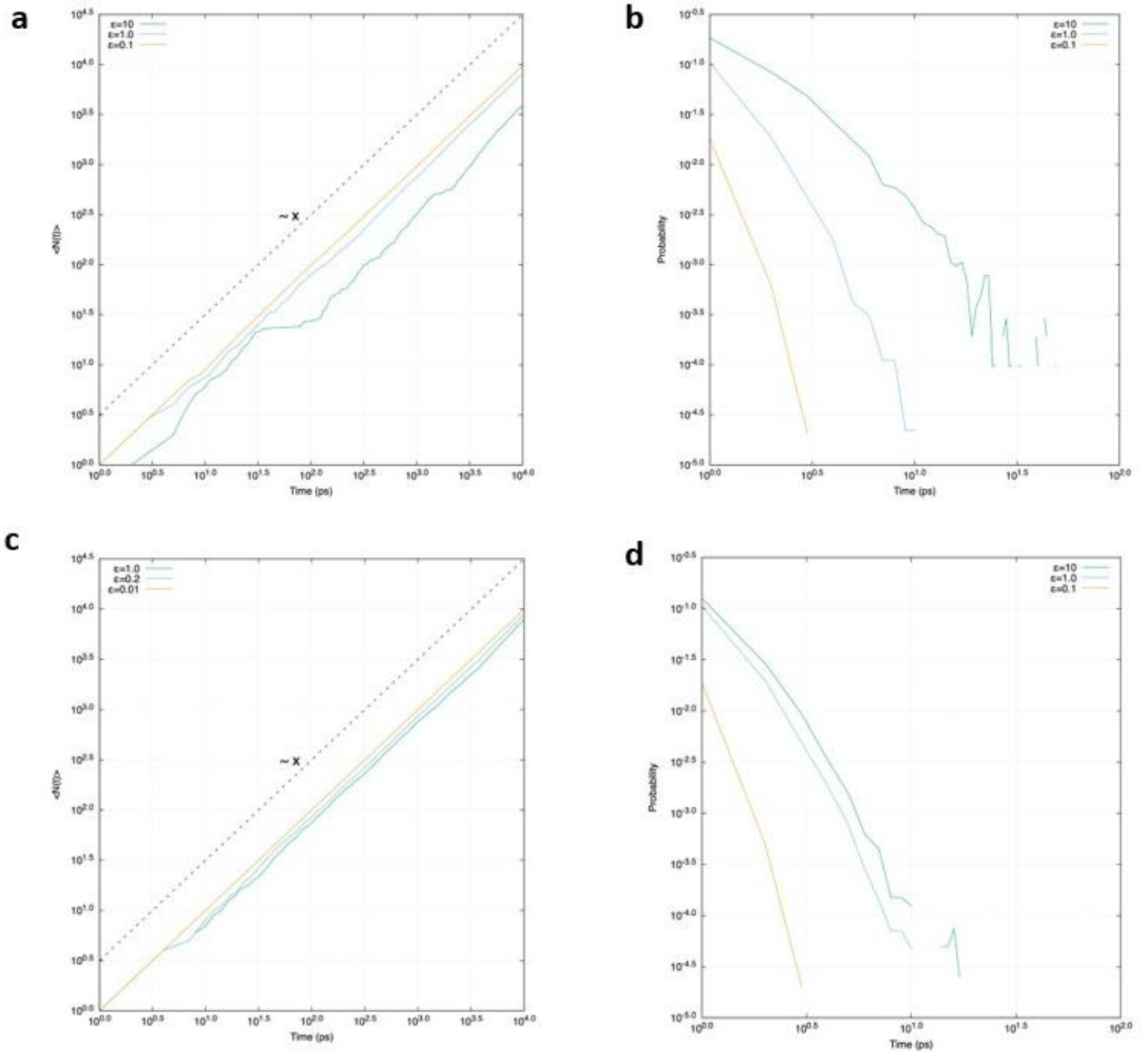


Fig. SI 2: $\langle N(t) \rangle$ and probability of jumps for H4 (a-b) and PDZ (c - d).

References:

- [1] K. Henzler-Wildman and D. Kern, *Dynamic Personalities of Proteins*, Nature **450**, 964 (2007).
- [2] A. Ansari, J. Berendzen, S. F. Bowne, H. Frauenfelder, I. E. Iben, T. B. Sauke, E. Shyamsunder, and R. D. Young, *Protein States and Proteinquakes.*, Proceedings of the National Academy of Sciences **82**, 5000 (1985).
- [3] S. D. Schwartz, *Protein Dynamics and Enzymatic Catalysis*, J Phys Chem B **127**, 2649 (2023).
- [4] Y. Wang, K. Bugge, B. B. Kragelund, and K. Lindorff-Larsen, *Role of Protein Dynamics in Transmembrane Receptor Signalling*, Curr Opin Struct Biol **48**, 74 (2018).
- [5] K. Bartels, T. Lasitzka-Male, H. Hofmann, and C. Löw, *Single-Molecule FRET of Membrane Transport Proteins*, ChemBioChem **22**, 2657 (2021).
- [6] L. Milanesi, J. P. Waltho, C. A. Hunter, D. J. Shaw, G. S. Beddard, G. D. Reid, S. Dev, and M. Volk, *Measurement of Energy Landscape Roughness of Folded and Unfolded Proteins*, Proceedings of the National Academy of Sciences **109**, 19563 (2012).
- [7] H. Frauenfelder, S. G. Sligar, and P. G. Wolynes, *The Energy Landscapes and Motions of Proteins*, Science (1979) **254**, 1598 (1991).
- [8] H. Yang, G. Luo, P. Karnchanaphanurach, T.-M. Louie, I. Rech, S. Cova, L. Xun, and X. S. Xie, *Protein Conformational Dynamics Probed by Single-Molecule Electron Transfer*, Science (1979) **302**, 262 (2003).
- [9] I. Grossman-Haham, G. Rosenblum, T. Namani, and H. Hofmann, *Slow Domain Reconfiguration Causes Power-Law Kinetics in a Two-State Enzyme*, Proceedings of the National Academy of Sciences **115**, 513 (2018).
- [10] G. Luo, I. Andricioaei, X. S. Xie, and M. Karplus, *Dynamic Distance Disorder in Proteins Is Caused by Trapping*, J Phys Chem B **110**, 9363 (2006).
- [11] S. C. Kou and X. S. Xie, *Generalized Langevin Equation with Fractional Gaussian Noise: Subdiffusion within a Single Protein Molecule*, Phys Rev Lett **93**, 180603 (2004).
- [12] Y. Wang and H. P. Lu, *Bunching Effect in Single-Molecule T4 Lysozyme Nonequilibrium Conformational Dynamics under Enzymatic Reactions*, J Phys Chem B **114**, 6669 (2010).
- [13] I. E. T. Iben et al., *Glassy Behavior of a Protein*, Phys Rev Lett **62**, 1916 (1989).
- [14] T. Neusius, I. Daidone, I. M. Sokolov, and J. C. Smith, *Subdiffusion in Peptides Originates from the Fractal-Like Structure of Configuration Space*, Phys Rev Lett **100**, 188103 (2008).
- [15] Y. Meroz, V. Ovchinnikov, and M. Karplus, *Coexisting Origins of Subdiffusion in Internal Dynamics of Proteins*, Phys Rev E **95**, 062403 (2017).
- [16] C. Xia, X. He, J. Wang, and W. Wang, *Origin of Subdiffusions in Proteins: Insight from Peptide Systems*, Phys Rev E **102**, 062424 (2020).
- [17] X. Hu, L. Hong, M. Dean Smith, T. Neusius, X. Cheng, and J. C. Smith, *The Dynamics of Single Protein Molecules Is Non-Equilibrium and Self-Similar over Thirteen Decades in Time*, Nat Phys **12**, 171 (2016).

- [18] S. Havlin and D. Ben-Avraham, *Diffusion in Disordered Media*, Adv Phys **51**, 187 (2002).
- [19] M. T. Barlow, *Diffusions on Fractals*, Lectures on Probability Theory and Statistics: Ecole d'Été de Probabilités de Saint-Flour XXV—1995 1 (2006).
- [20] C. J. McKnight, P. T. Matsudaira, and P. S. Kim, *NMR Structure of the 35-Residue Villin Headpiece Subdomain*, Nat Struct Biol **4**, 180 (1997).
- [21] G. Kozlov, D. Banville, K. Gehring, and I. Ekiel, *Solution Structure of the PDZ2 Domain from Cytosolic Human Phosphatase HPTP1E Complexed with a Peptide Reveals Contribution of the B2–B3 Loop to PDZ Domain–Ligand Interactions*, J Mol Biol **320**, 813 (2002).
- [22] R. K. Bijral, J. Manhas, and V. Sharma, *Hierarchical Clustering Based Characterization of Protein Database Using Molecular Dynamic Simulation*, in (2022), pp. 427–437.
- [23] S. Alexander, J. Bernasconi, W. R. Schneider, and R. Orbach, *Excitation Dynamics in Random One-Dimensional Systems*, Rev Mod Phys **53**, 175 (1981).
- [24] E. Suárez, R. P. Wiewiora, C. Wehmeyer, F. Noé, J. D. Chodera, and D. M. Zuckerman, *What Markov State Models Can and Cannot Do: Correlation versus Path-Based Observables in Protein-Folding Models*, J Chem Theory Comput **17**, 3119 (2021).
- [25] I. M. Sokolov, *Models of Anomalous Diffusion in Crowded Environments*, Soft Matter **8**, 9043 (2012).
- [26] B. Hess, H. Bekker, H. J. C. Berendsen, and J. G. E. M. Fraaije, *LINCS: A Linear Constraint Solver for Molecular Simulations*, J Comput Chem **18**, (1997).
- [27] H. J. C. Berendsen, J. P. M. Postma, W. F. Van Gunsteren, A. Dinola, and J. R. Haak, *Molecular Dynamics with Coupling to an External Bath*, J Chem Phys **81**, (1984).
- [28] D. J. Evans and B. L. Holian, *The Nose-Hoover Thermostat*, J Chem Phys **83**, (1985).
- [29] M. Parrinello and A. Rahman, *Polymorphic Transitions in Single Crystals: A New Molecular Dynamics Method*, J Appl Phys **52**, (1981).
- [30] M. J. Abraham, T. Murtola, R. Schulz, S. Páll, J. C. Smith, B. Hess, and E. Lindah, *Gromacs: High Performance Molecular Simulations through Multi-Level Parallelism from Laptops to Supercomputers*, SoftwareX **1–2**, (2015).
- [31] F. Pedregosa et al., *Scikit-Learn: Machine Learning in Python*, Journal of Machine Learning Research **12**, 2825 (2011).